

# Partitioning of ecosystem respiration in a beech forest

**Brændholt, Andreas; Ibrom, Andreas; Larsen, Klaus Steenberg; Pilegaard, Kim**

*Published in:*
Agricultural and Forest Meteorology

*Link to article, DOI:*
10.1016/j.agrformet.2018.01.012

*Publication date:*
2018

*Document Version*
Peer reviewed version

# Title

**Partitioning of ecosystem respiration in a beech forest**

Andreas Brændholt[1*], Andreas Ibrom[1], Klaus Steenberg Larsen[1,2] and Kim Pilegaard[1]

[1]DTU Environment, Technical University of Denmark; [2]Department of Geosciences and Natural Resource Management, University of Copenhagen.

*Correspondence author at: Bygning 115, Bygningstorvet, 2800 Kongens Lyngby, Denmark. E-mail address: andbr@env.dtu.dk

# ABSTRACT

Terrestrial ecosystem respiration ($R_{eco}$) represents a major component of the global carbon cycle. It consists of many sub-components, such as aboveground plant respiration and belowground root and microbial respiration, each of which may respond differently to abiotic factors, and thus to global climate change. To correctly predict future carbon cycles in forest ecosystems, $R_{eco}$ must therefore be partitioned and understood for each of its various components.

In this study we used the eddy covariance technique together with manual and automated closed-chambers to quantify the individual components of $R_{eco}$ in a temperate beech forest at diel, seasonal and annual time scales. $R_{eco}$ was measured by eddy covariance while respiration rates from soil, tree stems and isolated coarse tree roots were measured bi-hourly by an automated closed-chamber system. Soil respiration ($R_{soil}$) was measured in intact plots, and heterotrophic $R_{soil}$ was measured in trenched plots. Tree stem ($R_{stem}$) and coarse root ($R_{root}$) respiration were measured by custom made closed-chambers

We found that the contribution of $R_{stem}$ to total $R_{eco}$ varied across the year, by only accounting for 6 % of $R_{eco}$ during winter and 16 % during the summer growing season. In contrast $R_{soil}$ was approximately half of $R_{eco}$ during winter (52 %), spring (45 %) and summer (49 %), while the contribution increased to 79 % during autumn.

Based on observed fluxes in the trenched and intact soil plots, we found that autotrophic $R_{soil}$ accounted for 34 % of $R_{soil}$ during summer, i.e. a relatively low fractional estimate compared to findings from other studies. It is likely that dead roots were still decomposing in the trenched soil plots thus causing overestimation of heterotrophic $R_{soil}$.

Diel $R_{stem}$ and $R_{root}$ measurements showed a distinct pattern during summer with the highest respiration rates around 13:00-15:00 CET for $R_{stem}$, and the highest respiration seen from 9:00-15:00 for $R_{root}$. In contrast, $R_{soil}$ showed the lowest respiration during daytime with no clear difference in the diel pattern between the intact and trenched soil plots.

Finally, we calculated annual $R_{soil}$ for different transects, and found that annual $R_{soil}$ estimated from the previously used transect at the site was underestimated due to $R_{soil}$ of the transect not being representative for the spatial heterogeneity of $R_{soil}$ at the site. This highlights the importance of performing a sufficient number of chamber measurements at a site to adequately capture the spatial variation and estimate $R_{soil}$ correctly.

Keywords: Ecosystem respiration, flux partitioning, eddy covariance, chamber, seasonality

# 1 Introduction

Ecosystem respiration ($R_{eco}$) is, after gross primary productivity (GPP), the second largest flux of $CO_2$ between the biosphere and the atmosphere (Beer et al. 2010; IPCC, 2013). $R_{eco}$ is the sum of respiration from several component of the ecosystem that may respond differently to abiotic factors,

48 and thus to global change (Schimel et al., 2001; Valentini et al., 2003). To correctly understand and
49 predict future ecosystem carbon cycles, $R_{eco}$ must therefore be partitioned into its main sub-
50 components. For forests, major components are aboveground autotrophic respiration from the
51 leaves, branches and stems of the trees, and belowground by the autotrophic respiration from tree
52 roots and the heterotrophic respiration from soil microbes, which together form the soil respiration
53 ($R_{soil}$) (Hanson et al., 2000; Högberg et al. 2005, Rodeghiero and Cescatti, 2006).
54 Ecosystem-level net atmospheric exchange of $CO_2$ (NEE) can be measured on a high temporal
55 scale by the eddy covariance method (e.g. Pilegaard et al., 2001; Wofsy et al., 1993). NEE can be
56 partitioned into GPP and $R_{eco}$, by various extrapolation methods, one of which uses temperature
57 response functions to extrapolate from measured nighttime respiration rates to estimates of daytime
58 respiration (Reichstein et al., 2005). Whereas eddy covariance provides $R_{eco}$ on a high temporal
59 scale, it does not provide information on the individual components that make up $R_{eco}$. Instead,
60 chamber based methods can be used to measure the $CO_2$ flux from the individual components by
61 enclosing a specific part of the ecosystem in a chamber. Typically, chambers of the closed type are
62 used, where the $CO_2$ flux is calculated based on the near-linear increase in chamber $CO_2$
63 concentration during the measurement. Chamber-based methods differ from the eddy covariance
64 method by the smaller spatial coverage (Wang et al., 2010). Eddy covariance covers a large
65 footprint area that may be representative for the studied ecosystem (Nagy et al., 2006). $R_{soil}$,
66 however, often show a high degree of spatial heterogeneity within the footprint area (Knohl et al.,
67 2008; Webster et al., 2008). At eddy covariance sites, $R_{soil}$ is often determined with manually
68 operated soil chambers (e.g. Wu et al., 2013). To ensure that $R_{soil}$ measurements are representative
69 for the eddy covariance footprint, a sufficient number of measurements must be performed
70 throughout the footprint (Davidson et al., 2002; Savage et al., 2008). By performing the manual
71 chamber measurements distributed throughout the footprint at regular intervals throughout the year,

72 both the seasonal change in $R_{soil}$ and the spatial difference in $R_{soil}$ can be captured to give a good
73 estimate of $R_{soil}$ for the footprint (Savage and Davidson, 2003). However, because of labour
74 intensiveness, manual measurement campaigns rarely capture diel or day to day variability in the
75 fluxes. Automated chamber systems can allow for measurements at much higher temporal
76 resolution, but because of budget constraints usually only a limited number of automated chambers
77 are available causing low spatial coverage of automatic systems. Apart from $R_{soil}$, measurements of
78 other ecosystem components such as respiration from leaves, branches and tree stems and woody
79 debris lying on the soil surface have been made using both manual and automated chambers
80 (Rodríguez-Calcerrada et al., 2014; Tang et al., 2008; Zhu et al., 2012). As for $R_{soil}$, these
81 components can show a high degree of spatial and temporal variability throughout the footprint,
82 thus requiring a sufficient number of chamber measurements to capture this variability.
83 The diel pattern of $R_{soil}$ is generally related to soil temperature (Janssens and Pilegard, 2003; Tang
84 et al., 2005). However, differences in substrate input of carbon from photosynthesis to the soil via
85 the roots can vary across the day (Kuzyakov and Gavrichkova, 2010). Diel changes in substrate
86 input from plants may completely or partly decouple $R_{soil}$ from the diel pattern of soil temperature
87 (Tang et al., 2005). To study the influence of substrate input and the autotrophic contribution from
88 roots to $R_{soil}$, a trenching can be performed. Here the contribution of roots to $R_{soil}$ is removed by
89 cutting off any roots in a plot and preventing them to grow back (Baggs, 2006; Bond-Lamberty et
90 al., 2011). This stops autotrophic $R_{soil}$ and prevents any input of carbon from photosynthesis.
91 However, the roots are left to decay in the plot and the soil water content may increase (Díaz-Pinés
92 et al., 2010). By comparing plots with intact soil to plots with trenched soil, the heterotrophic and
93 autotrophic components of $R_{soil}$ can be investigated.
94 The aim of the study was to quantify the $CO_2$ fluxes from various components of a forest ecosystem
95 on an annual, seasonal, daily and diel scale, and to quantify how the contribution to total $R_{eco}$ of

heterotrophic and autotrophic $R_{soil}$ and stem respiration ($R_{stem}$) vary on a seasonal scale. This was achieved by a combination of the eddy covariance method and manual and automated closed-chamber techniques.

# 2 Materials and Methods

## 2.1 Site description

Measurements were performed at the Danish ICOS RI site called DK-Sor at 40 m a.s.l. (55°29'13'' N, 55°38''45'' E), where eddy covariance measurements of net ecosystem $CO_2$ fluxes have been performed continuously since 1996. The climate is temperate maritime with an annual average precipitation and an annual average temperature of 564 mm and 8.5 °C, respectively (Pilegaard et al. 2011).

The forest is dominated by European beech (*Fagus sylvatica* L.) planted in 1921 with small stands of Norway spruce (*Picea abies* (L.) Karst) and European larch (*Larix decidua* Mill.) (Wu et al. 2013). The tree stem density is 288 per hectare with an average tree height of 28 m and an average diameter at breast height (DBH) of 42 cm in 2010. The main rooting depth is 1 m (Pilegaard et al. 2011). However, roots are most frequent at a depth of 0-20 cm (Østergård, 2001). The dense canopy has a peak LAI of 5.0 and the average annual canopy cover duration period is 180 days. The understory is poorly developed due to the well-developed canopy, causing a sparsely vegetated forest floor during most of the year, except during spring when wood anemones (*Anemone nemorosa* L.) are present in part of the forest floor. Depending on the base saturation, the soils are classified as either alfisols or mollisols. The soil carbon pool is 20 kg $m^{-2}$ down to 1 m depth, with a C/N ratio of 20 in the upper organic soil layers, decreasing to 10 in the lower mineral layers (Østergård, 2001). The organic layer is 10–40 cm deep (Pilegaard et al. 2001).

## 2.2 Eddy covariance measurements

Measurements of NEE were performed at a height of 43 m on the flux tower on the site by a closed-path eddy covariance system based on a Gill HS-50 3D research sonic anemometer (Gill Instruments Limited, Lymington, UK) and a fast response infrared gas analyser LI-7000 (LI-COR Environmental, Lincoln, Nebraska, USA). For details on the raw data processing, see Pilegaard et al. (2011). Nighttime fluxes at insufficient turbulent mixing were removed when the friction velocity ($u_*$) was lower than 0.1 m $s^{-1}$ and the atmospheric stratification was stable. A dead band of 2 hours after re-establishment of turbulent conditions was applied to avoid double accounting from measuring $CO_2$ fluxes from venting the canopy air space. The removal of data below the $u_*$ threshold value, and periods of system failure, resulted in a data coverage of 54.1 % for 2016. The data set was gap-filled and NEE was partitioned into GPP and $R_{eco}$ by the online "REddyProc: Eddy covariance data processing tool" (Department of Biogeochemical Integration, MPI Jena). In short, the gap-filling procedure follows the approach by Reichstein et al. (2005), and the partitioning of NEE follows the look-up table approach by Reichstein et al. (2005) and the regression approach by Lasslop et al. (2010). This resulted in a continuous data set of half-hourly values of NEE, GPP and $R_{eco}$ for the entire year. From the half-hourly values, the mean daily values were calculated as well as monthly and annual sums of NEE, GPP and $R_{eco}$.

For the each of the annual sums of NEE, GPP and $R_{eco}$ an uncertainty estimate was calculated. Wu et al. (2013) used five years of data to calculate the relative uncertainties of the annual sums of NEE, GPP and $R_{eco}$ for the DK-Sor site by taking the uncertainties caused by $u_*$ filtering, gapfilling and site heterogeneity into account. By using these relative uncertainties, we calculated the uncertainty estimates for the annual sums of NEE, GPP and $R_{eco}$.

### 2.3 Manual closed-chamber soil respiration measurements

143 $R_{soil}$ was measured manually using a portable 8100-102 10 cm survey chamber connected to a LI-
144 8100A Automated Soil $CO_2$ Flux System (LI-COR Environmental, Lincoln, Nebraska, USA). $R_{soil}$
145 was measured on permanently installed soil collars, inserted 4 cm into the soil, on three distinct
146 transects in the footprint area of the eddy covariance measurements. The $R_{soil}$ plots contained litter
147 but no living plants. The first transect, called the inside fence transect, consisted of 12 plots that
148 were positioned within 15 m of the flux tower. The second transect, called the south transect,
149 consisted of 27 plots, which were positioned at 9 locations along a straight line starting 30 m from
150 the flux tower and ending 270 m south of the tower. Each of the 9 locations contained 3 $R_{soil}$ plots.
151 The last transect, called the west transect, consisted of 45 plots. The plots were positioned in groups
152 of three at 15 locations along two parallel lines that were separated by 30 meters. The lines started
153 30 m from the flux tower and ended 210 m to the west. The location for the south and west transects
154 were chosen to be in the main wind directions and source area for the eddy covariance
155 measurement. See Pilegaard et al. (2011) and Wu et al. (2013) for information about the footprint
156 area and wind direction at the site.
157 The manual measurements were performed at an interval of two to three weeks, where $R_{soil}$ was
158 measured once per plot with a chamber closure time of 150 seconds. This resulted in 20 campaign
159 measurements evenly distributed in time during 2016 for each of the transects. The measurements
160 of the three transects were typically performed on two adjacent days between 09:00–16:00 CET,
161 with the inside fence and south transect being measured on the first day, and the west transect being
162 measured on the second day.
163
164 **2.4 Automated closed-chamber measurements**
165 In addition to the manual chamber measurements, automated closed-chamber measurements of
166 respiration from intact soil, trenched soil, coarse roots and tree stems were performed from 4

January 2016 to 31 December 2016 with a LI-8100A Automated Soil $CO_2$ Flux System connected to a LI-8150 Multiplexer (LI-COR Environmental, Lincoln, Nebraska, USA). All the automated soil, root and stem chambers were positioned within 15 m from the flux tower. The system performed well through the entire measurement period leading to automatic measurement being performed each day.

$R_{soil}$ was measured by six opaque soil chambers on circular soil collars with a diameter of 20 cm that were permanently inserted 4 cm into the soil. The soil collars contained soil and litter but no aboveground plant parts. One of the soil chambers was an 8100-101 Long-Term $CO_2$ flux chambers, and five were 8100-104 Long-Term $CO_2$ flux chambers (LI-COR Environmental, Lincoln, Nebraska, USA). For two of the soil chambers, trenching was first performed on 6 April 2016 to remove the contribution of living roots to the total $R_{soil}$ from the plot. The trenching was done by vertically inserting a spade 25 cm into the soil in a circle around the soil chambers. Roots with a diameter too big to be cut with the spade were cut with a saw. To prevent ingrowth of roots, monthly re-trenching was performed throughout the study period. Thus, the six soil chamber plots consisted of two trenched soil plots and four intact soil plots.

$R_{stem}$ and $R_{root}$ were measured with two custom made coarse root chambers and two custom made stem chambers, respectively. Unlike the LI-COR soil chambers, the root and stem chambers did not open between measurements. Instead, the chamber headspace was continuously flushed between measurements with atmospheric air that was let into the chamber by a small tube. The flow of air to all root and stem chambers was provided by a pump, and the flow to each chamber set to 1 L $min^{-1}$ by a flow meter. This resulted in a near ambient atmospheric air $CO_2$ concentration in the chambers between measurements. At the beginning of a chamber measurement, the flow of air to the specific chamber was stopped by automatically closing a normally open solenoid valve that was placed on the flush tube going to the chamber. Thus, the chambers were closed during measurements.

191 The two root chambers were made of transparent acrylic glass and were cylindrical in shape with an
192 inner length of 24 cm and an inner diameter of 7 cm giving a volume of 923 $cm^3$. Before assembly
193 the cylinder was cut in two halves in the longitudinal axis. A 10 cm long tube with an inner
194 diameter of 0.5 cm, and a filter in the end was attached to the chamber, which acted as a vent to the
195 atmosphere. The chambers were installed in June 2015. For each chamber a suitable coarse root
196 from a soil depth of 5-10 cm was carefully exposed, and the root was rinsed by tap water. The
197 diameter of root was measured, and the root volume and root surface area was calculated. The root
198 was placed in the one half of the cylinder and the other half of the cylinder was placed on top. In
199 each end of the cylinder, the root went through a hole. The two half cylinders were sealed to each
200 other and the hole around the root in each end was sealed with Blu-tack. Following this, the
201 chamber was covered with soil.
202 The two stem chambers were cylindrical and made of polypropylene, with an inner diameter of 15
203 cm and an inner height of 10 cm, giving a volume of 1757 $cm^2$. A 10 cm vent tube with an inner
204 diameter of 0.5 cm, and a filter in the end was attached at the bottom of the chamber. The chambers
205 were attached to the smooth stem surfaces of two beech trees at a height of 1.3 m by a rubber
206 extrusion with a u-profile that was attached to the chamber and sealed with silicone. The chamber
207 was held in place on the stem by adjustable straps.
208 The ten chambers were connected to the LI-8100A/ LI-8150 in a multiplexed setup, and the system
209 was set up in a repeated automated two-hour cycle during which a measurement of each of the soil,
210 root and stem chambers was performed. The chamber closure time was set to 5 minutes and the pre-
211 purge and post-purge times were set to 40 seconds for all chambers.
212
213 **2.5 Chamber flux calculation and up-scaling of fluxes**

All data analysis of the chamber based $CO_2$ fluxes and post-processing of the eddy covariance data was done using R version 3.2.0 (R Core Team, 2014).

$CO_2$ fluxes for all chamber measurements were calculated for each individual measurement on a time and area basis by fitting the non-linear equation by Hutchinson and Mosier (1981) with the nlsLM function (minpack.lm package) for model fitting in R (Elzhov et al. 2015). For the manual chamber measurements, the first 20 seconds after chamber closure were discarded from the flux calculation (the dead band), whereas the dead band was set to 100 seconds for the automated chamber measurements because an external analyser (used in another study) was attached in parallel with the LI-8100/LI-8150 system, causing increased system volume and therefore increased system response time.

The calculated automated chamber fluxes from soil, stem and coarse roots were quality flagged first by removing fluxes with an $r^2 < 0.80$ of the fit. Following this, the automated soil fluxes, but not stem and root fluxes, were further quality flagged by removing measurements performed at low $u_*$, where soil fluxes measured by the LI-8100A/LI-8150 system at the site have been found to be overestimated (Brændholt et al. 2017). In short, the automated soil chamber fluxes were compared with $u_*$ measured at the flux tower. From a plot of the fluxes against $u_*$, a threshold value of 0.2 m $s^{-1}$ was determined visually, as where the decrease of fluxes in response to an increase in $u_*$ levelled off. Fluxes below the $u_*$ threshold value were removed from further analysis. In total the quality control removed 16.3 % of the automated root and stem chamber measurements and 44.9 % of the automated soil chamber measurements, leaving 30124 automated chamber measurements for further analysis. For the manual chamber measurements no quality control was applied in the post processing. Instead the quality control was done in the field following a measurement. If the coefficient of variance of the flux, provided by the LI-COR software, was higher than 1.4 %, the measurement was discarded and an extra measurement was performed on the plot.

From the quality controlled flux chamber measurements different estimates for the annual $CO_2$ fluxes were calculated for both the manual and automated measurements following the procedure described by Brændholt et al. (2017). For the manual measurements, annual soil $CO_2$ fluxes were calculated both for the inside fence transect, the south transect and the west transect.

For each transect, the manual fluxes were used to parameterize an empirical model of $R_{soil}$ as a function of soil temperature as described by Lloyd and Taylor (1994):

$$R_s = R_{283} \exp\left[-E_0\left(\frac{1}{T_s+273.15-T_0} - \frac{1}{T_s-T_0}\right)\right], \quad (1)$$

where $T_0$ and $E_0$ are fitted parameters, $T_s$ is soil temperature measured at 5 cm depth and $R_{283}$ is the base respiration at a soil temperature of 10 °C. The model was fitted with nlsLM in the R package minpack.lm (Elzhov et al. 2015) that uses a nonlinear least squares regression based on a Levenberg–Marquardt algorithm. By using soil temperature at 5 cm depth measured continuously at the site as model driver input, a continuous one-year time series of mean daily $R_{soil}$ was calculated. A potential soil temperature bias could occur if the soil temperature continuously measured inside the fence at the site, which was used for modelling of the annual $CO_2$ fluxes, systematically differed from the soil temperatures of the manually measured soil respiration plots. However, no systematic soil temperature difference was found, e.g. exemplified by a mean annual soil temperature inside the fence of 8.4 °C compared to mean annual soil temperatures of 8.7 and 8.2 °C for the south transect and west transect, respectively.

For the automated measurements, annual mean $CO_2$ fluxes were calculated for the four intact soil plots, the two trenched soil plots, the two root plots and the two stem plots, respectively. Each of the annual $CO_2$ fluxes was calculated by first averaging the bi-hourly fluxes on a monthly basis, providing a diel pattern of fluxes for each month. From this, a daily mean flux was calculated on a

monthly basis at the average of the bi-hourly values. Monthly fluxes were calculated as the sum of the daily soil fluxes in the respective month, and the annual flux was calculated as the sum of the 12 months.

The uncertainties of the annual soil $CO_2$ fluxes based on the manual chamber for each of the three transects were estimated by the approach used in Wu et al. (2013), which is based on Van Oijen et al., (2005). In short, for each transect a Bayesian calibration was used to quantify the uncertainty of the model predictions, for which a Markov Chain Monte Carlo (MCMC) Metropolis-Hastings random walk algorithm was used. We performed 50000 MCMC iterations from which the prior parameter distributions were sampled. Different annual soil $CO_2$ fluxes were calculated using the estimated posterior parameter distributions, and the standard deviation of the annual soil $CO_2$ fluxes was interpreted as the uncertainty of the annual soil $CO_2$ flux for a given transect.

$R_{stem}$, calculated on a stem surface area, was scaled up to the soil surface area by using site data on tree density, tree height and DBH. The tree height and DBH were measured for 54 beech trees during March 2017. For each of the measured trees, the surface stem area was calculated as the surface area of a cylinder with the measured height and a diameter of 0.71 times the measured DBH. This diameter was derived from a form factor for European beech that describes the relationship between the stem ground area at breast height and the volume of wood contained in the stem and branches above a diameter of 5 cm (Landesverwaltungsamt Sachsen-Anhalt). The average stem surface area calculated from the sampled trees was multiplied with the tree density of 288 stems $ha^{-1}$ to get the stem surface area scaled on a soil surface area. From this the measured $R_{stem}$ on a stem surface area could be converted to a $CO_2$ flux on a soil surface area.

The uncertainties of the annual soil $CO_2$ fluxes for the intact soil, trenched and stem measured by the automated chamber were estimated by formal error propagation that took the uncertainties of the various steps in the calculation of the annual fluxes into account. For the annual stem flux, an extra

level of uncertainty was included in the calculation that accounted for the uncertainty of the up-scaling of the fluxes from stem surface area to soil surface area. For this, we assumed an uncertainty of 30 % in the stem surface area calculated from the measurements of tree height and DBH.

# 3 Results

## 3.1 Annual $CO_2$ budgets

Different annual $CO_2$ budgets were calculated for different components of the forest from both the tower based eddy covariance and the automated and manual closed-chamber measurements.

The gap-filled annual NEE calculated from the eddy covariance measurement at a height at 43 m on the flux tower was -391 ± 63 g C $m^{-2}$ $yr^{-1}$, and the estimated GPP and $R_{eco}$ were 2272 ± 136 and 1882 ± 301 g C $m^{-2}$ $yr^{-1}$, respectively (Fig. 1).

Different estimates of annual $R_{soil}$ were calculated based on the manual closed-chamber measurements that were used to parameterize the Lloyd and Taylor model (Fig. 1). The lowest annual $R_{soil}$ of 794 ± 51 g C $m^{-2}$ $yr^{-1}$ was found for the inside fence transect, where the plots were positioned within a distance of 15 m from the eddy flux tower. The annual $R_{soil}$ from the two transects, with soil plots distributed in the forest, were both higher with an annual $R_{soil}$ of 1024 ± 89 g C $m^{-2}$ $yr^{-1}$ for the west transect and an annual $R_{soil}$ of 972 ± 90 g C $m^{-2}$ $yr^{-1}$ for the south transect.

The average annual $R_{soil}$ based on the automated closed-chamber measurements every two hours was 597 ± 93 g C $m^{-2}$ $yr^{-1}$ for the four automated chambers with intact soil and, while the average annual $R_{soil}$ for the two automated chambers containing trenched soil was 375 ± 29 g C $m^{-2}$ $yr^{-1}$, accounting for 63 % of $R_{soil}$ for the intact soil plots.

The annual up-scaled stem $CO_2$ on a soil surface area basis was 264 ± 88 and 191 ± 64 g C $m^{-2}$ $yr^{-1}$ for the two automated stem chambers, respectively, resulting in an average of 227 ± 108 g C $m^{-2}$ $yr^{-1}$ (Fig. 1). This was equivalent to 258 ± 15 g C $m^{-2}$ $yr^{-1}$ on a stem surface area basis.

310 Compared to the annual estimate of $R_{eco}$ from the eddy covariance measurements, the annual $R_{soil}$
311 constituted 43, 55 and 52 % from the manually measured inside fence transect, the west transect and
312 the south transect, respectively, while the annual $R_{soil}$ based in the intact soil plots and trenched soil
313 plots measured automatically constituted 32 and 20 % of $R_{eco}$, respectively. The average stem $CO_2$
314 flux constituted 12 % of $R_{eco}$.
315
316 **3.2 Seasonal forest respiration**
317 $R_{eco}$, $R_{soil}$ and $R_{stem}$ generally followed the same pattern throughout the year with the lowest
318 respiration rates during the cold winter months and the highest rates during the warm summer
319 months (Fig. 2, Fig. 3). However, the individual contribution of $R_{soil}$ and $R_{stem}$ to the total $R_{eco}$
320 differed between the seasons. $R_{stem}$ showed a high seasonality in its contribution to the total $R_{eco}$
321 contributing only 6 % of $R_{eco}$ during the winter months of January, February and December. A
322 similar low contribution of 7 % was seen during the spring months of March, April and May.
323 However, during the summer months of June, July and August the contribution of $R_{stem}$ increased to
324 16 %. In the autumn months of September, October and November the contribution gradually
325 decreased from 16 % in September to a level of 9 % in November, close to the winter level. The
326 monthly pattern of contribution of $R_{soil}$ to the total $R_{eco}$ differed from $R_{stem}$. Here winter, spring and
327 summer were fairly similar contributing 52, 45 and 49 % to $R_{eco}$, respectively. However, $R_{soil}$ during
328 the autumn months differed from the rest of the year by contributing 79 % to the total $R_{eco}$.
329 $R_{root}$, which was measured for two coarse roots, was not scaled up to the soil surface area because of
330 the various contributions of roots of different sizes to total root respiration.
331
332 **3.3 Effect of trenching**

The annual average $R_{soil}$ for the two trenched soil plots measured by the automated chambers was 63 % of annual average $R_{soil}$ for the four intact soil plots. However, the trenching was not performed until 5 April 2016. To investigate the effect of the trenching on $R_{soil}$, we looked at $R_{soil}$ before and after the trenching. Before the trenching $R_{soil}$ of the trenched plots was 77 % of the $R_{soil}$ for the intact soil. However, for the remaining part of the year following the trenching, $R_{soil}$ for the trenched plots decreased to 61 % of the intact soil plots.

The course of $R_{soil}$ generally followed the same pattern throughout the year for both the intact and trenched soil plots, by following changes in soil temperature (Fig. 3). However, during the months of June, July and August where GPP was highest (Fig. 4), the intact soil plots reached higher levels of $R_{soil}$ with $R_{soil}$ of the trenched soil plots only being 51 % of the intact plots. $R_{soil}$ of one of the intact soil plots differed by showing a rapid increase in $R_{soil}$ during April and May, but then decreasing again to a level similar to the remaining intact soil plots (Fig. 3). For October, November and December during autumn and winter, where GPP was low to near zero μmol $m^{-2}$ $s^{-1}$, $R_{soil}$ of the intact soil plots decreased to almost the level of the trenched soil plots, with $R_{soil}$ of the trenched plots being 83 % of the intact plot, a higher level than the pre-trenching level of 77 %.

### 3.4 Stem respiration and GPP

A rapid increase in GPP was seen in May following the leaf out of the deciduous beech trees (Fig. 4). GPP peaked in June and the high GPP continued into July, following by lower GPP in August and September. A similar rapid increase in May was not seen for the two $R_{stem}$ plots. Instead, a slower increase was seen in May followed by a peak in $R_{stem}$ in July and August. During autumn, however, the decrease in $R_{stem}$ did seem to follow the decrease in GPP. Instead of following GPP, the course of $R_{stem}$ followed the course of $R_{soil}$ during spring, summer and autumn (Fig. 4). However, during summer a higher day to day variability was seen for $R_{soil}$ compared to $R_{stem}$.

357

### 3.5 Diel patterns of $CO_2$ fluxes

The automated chamber measurements performed every two hours throughout the year allowed for investigating the diel patterns of $R_{stem}$, $R_{root}$ and $R_{soil}$ for both the trenched and intact soil plots for the different seasons of the year (Fig. 5).

Although $R_{soil}$ was higher for the intact soil plots than for the trenched plots, the diel pattern of $R_{soil}$ generally exhibited the same pattern for both the intact (Fig. 5a, b, c, d) and the trenched soil plots (Fig. 5a, b, c, d). During winter, $R_{soil}$ was generally higher during daytime than during nighttime. For spring and autumn, however, no clear diel pattern was observed. Summer exhibited a diel pattern with generally low $R_{soil}$ during daytime. A peak in $R_{soil}$ was seen early in the morning and late in the evening before midnight. The diel patterns of $R_{stem}$ and $R_{root}$ during summer differed from $R_{soil}$ by having the highest respiration rates during daytime (Fig. 5k, o). $R_{stem}$ peaked at 13:00-15:00 CET, while a longer peak period from 9:00-15:00 was seen for $R_{root}$. For winter and autumn, no diel pattern was seen for $R_{root}$ (Fig. 5i, l). However, during spring, a similar diel pattern as during summer with highest $R_{root}$ during daytime was observed. The diel pattern of $R_{stem}$ during spring and autumn was similar to the diel pattern during summer, although less pronounced, with highest $R_{stem}$ during daytime. $R_{stem}$ for winter, however, showed no diel pattern, which was in contrast to the high daytime $R_{stem}$ seen during the rest of the year.

Soil temperature at 5 cm depth generally showed no diel pattern during winter, summer and autumn (Fig. 6). During spring, however, a moderate diel pattern was observed with highest soil temperatures late in the afternoon or early in the evening and the lowest soil temperatures in the morning. The difference between the highest and lowest diel temperature was, however, only approximately 1 °C.

# 4 Discussion

## 4.1 Annual $R_{soil}$ at different transects

We measured $R_{soil}$ at three different transects, which revealed that the annual $R_{soil}$ measured on the inside fence transect was 20 % lower than the average annual $R_{soil}$ measured on the west and south transects. Manual $R_{soil}$ measurements on the inside fence transect have previously been used on the site to estimate annual $R_{soil}$. Wu et al. 2013 found an average annual $R_{soil}$ of 752 ± 30 g C $m^{-2}$ $yr^{-1}$ for a 5 year period, which is close to the 794 ± 51 found in this study. They calculated the aboveground autotrophic respiration to 872 g C $m^{-2}$ $yr^{-1}$, which they found to be unexpectedly high. They argued that it could be explained if $R_{soil}$ had been underestimated, due to the plots having lower $R_{soil}$ than the average $R_{soil}$ of the footprint. The inside fence transect consisted of 12 plots all positioned within 15 meter of the flux tower, at a relatively dry and high ground. In contrast, the two newly established west and south transects, not used in Wu et al. (2013), consisted of 27 and 45 plots, respectively, that were spread out evenly in the forest. $R_{soil}$ and soil moisture measured at both transects showed a higher variation than $R_{soil}$ and soil moisture measured at the inside fence transect (Data not shown). Thus, we argue that the two new transects better represent the spatial variation of $R_{soil}$ in the eddy covariance footprint than the inside fence transect. The annual $R_{soil}$ for the two transects were, however, also similar (972 ± 90 and 1024 ± 89 g C $m^{-2}$ $yr^{-1}$), constituting 53 % of $R_{eco}$. Knohl et al. (2008) recommended using at least 8 measurement locations spaced randomly throughout the area of interest to get a representative estimate of $R_{soil}$ with sufficient confidence. The two new transects contained 9 and 15 locations throughout the eddy covariance footprint, respectively, each location containing 3 soil collars. Thus, measuring $R_{soil}$ on only one of these transects might be sufficient to cover the spatial variability and get a solid estimation of $R_{soil}$. The minor difference between the annual $R_{soil}$ from the two transects also supports this. In contrast, the

12 soil collars in the inside fence transect only cover 1 location because they are placed closely together, and therefore do not live up to the recommendations by Knohl et al. (2008).

If the new transects had been used in Wu et al. (2013), the higher $R_{soil}$ would have changed the extremely high estimate of aboveground autotrophic respiration. If we correct $R_{soil}$ in Wu et al. based on the relationship between $R_{soil}$ of the inside fence transect and the other two transects in this study, then the annual $R_{soil}$ increases from 752 to 945 C $m^{-2}$ $yr^{-1}$. This is turn would lower the estimate of aboveground autotrophic respiration from 872 to 679 g C $m^{-2}$ $yr^{-1}$, and make the estimates of above and belowground autotrophic respiration more similar as would be expected (Wu et al. 2013).

The annual $R_{soil}$ based on the automated closed-chamber measurements on the 4 intact soil plots was 597 ± 93 g C $m^{-2}$ $yr^{-1}$, lower than annual $R_{soil}$ of the 3 transects measured by manual chambers. The automated measurements were performed within 15 m from the flux tower, close to the 12 plots of the inside fence transect. Thus, a somewhat similar annual $R_{soil}$ could be expected. However, the annual $R_{soil}$ of the inside transect was 794 ± 51 g C $m^{-2}$ $yr^{-1}$, higher than the annual $R_{soil}$ based on the automated measurements. The cause for the difference in $R_{soil}$ is unknown. Even though the plots are positioned close to each other, it is possible that spatial heterogeneity within a few metres have caused the difference in $R_{soil}$. Another possibility is the different closed-chamber systems used, that potentially could lead to different absolute flux values. Lastly, it is possible that the difference between the day time only measurements for the manual chambers and the measurements every two hours for the automated chambers have caused the difference in $R_{soil}$.

### 4.2 Comparison of annual respiration

GPP was found to be 2272 ± 136 g C $m^{-2}$ $yr^{-1}$ (Fig. 1). This is high compared to the average of 1881 ± 127 g C $m^{-2}$ $yr^{-1}$ that has previously been found for the site (Wu et al. 2013). We expect an

optimal growing season during the study period to be part of the reason for this. No summer drought was observed, which has been found to lower forest growth during summer, thus lowering annual GPP (Ciais et al., 2005). The trees could therefore continue to photosynthesize without any edaphic or climatic reduction during summer. Furthermore, September was exceptionally warm, which allowed the trees to continue photosynthesizing for an additional period at high rates (Fig. 4). $R_{eco}$ was found to be high as well at 1882 ± 301 g C $m^{-2}$ $yr^{-1}$, which is to be expected due to the commonly found link between GPP and $R_{eco}$ (Mahecha et al., 2010; Peichl et al., 2013) and higher than the 1624 ± 201 g C $m^{-2}$ $yr^{-1}$ found by Wu et al. (2013). Luyssaert et al. (2007) assembled a global database of GPP and $R_{eco}$ and reported the average GPP and $R_{eco}$ to be 1375 ± 56 and 1048 ± 64, respectively, for temperate humid deciduous forests, which is much lower than found for the DK-Sor forest. However, we expect GPP and $R_{eco}$ for the DK-Sor forest to be higher because the forest is at its main productive phase with a uniform stand of 100 year-old beech trees with high LAI and a fertile soil. Furthermore, the mild maritime climate and the moderately high latitude close to the northern margin of beech forest's geographic range have relatively long days during the vegetation period. With a canopy process model, Ibrom et al. (2006) showed for two different conifer canopies that the northern, maritime climate in Scotland increased the photosynthetically active radiation use efficiency by 13-14 % compared to a more continental climate at a forest site in Central Germany. The reason was longer day lengths, a higher fraction of diffuse radiation and lower vapour pressure deficit at the Scottish site. Compared to the main beech distribution area with many drier and more continental sites, we conclude that the site conditions at the DK-Sor beech forest site allow for comparably high forest productivity.

We found an average annual $R_{stem}$ per unit ground area of 227 ± 108 g C $m^{-2}$ $yr^{-1}$, which is the first estimate for this flux component at this site (Fig. 1). The quantification of the $CO_2$ flux from tree stems has not received the same attention as e.g. $R_{soil}$ and $R_{eco}$, probably associated with the extra

452 work and cost required to construct and operate the custom made stem chambers, and the
453 complications to upscale the measurements to the total stand level. $R_{stem}$ can, however, be a
454 substantial part of $R_{eco}$, and constituted 12 % of $R_{eco}$ in our study. A few studies have addressed the
455 role of $R_{stem}$ for different forest ecosystems (Ceschia et al., 2002; Edwards and Hanson, 1996;
456 Inoue, 2004; Saveyn et al., 2007; Yang et al., 2015; Zha et al., 2004), and a few studies have looked
457 at $R_{stem}$ for beech trees (Ceschia et al., 2002; Damesin et al., 2012; Saveyn et al., 2007). Tang et al.
458 (2008) found that $R_{stem}$ accounted for 13 % of $R_{eco}$ in a temperate old-growth hardwood forest in the
459 USA, close to the findings for our forest. Damesin et al. (2002) measured respiration from stem and
460 branches and estimated the annual respiration to be between 325 and 383 g C $m^{-2}$ $yr^{-1}$, with $R_{stem}$
461 accounting for approximately 50 %. In a review of 18 European forests, Janssens et al. (2000) found
462 that aboveground respiration accounted for 31 % of $R_{eco}$. If half of the aboveground respiration is
463 accounted for by $R_{stem}$ as found by Damesin et al. (2002), then 12 % of $R_{eco}$ accounted for by $R_{stem}$ in
464 our study is close to the findings by Janssens et al. (2000).
465 Upscaling $R_{stem}$ from chamber based measurements to soil surface area for comparison with other
466 ecosystem respiration components can cause considerable up-scaling biases. Three main causes of
467 errors can be identified: Insufficient number of measurements in time to catch the temporal
468 resolution in $R_{stem}$, insufficient number of measurements to catch the spatial variability in $R_{stem}$
469 between and within trees, and uncertainty related to scaling up surface measurements to the entire
470 surface of the tree stand. The automatic stem chambers ran continuously throughout the year, thus
471 capturing even the hourly variation of $R_{stem}$. However, only two stem chambers were available.
472 Annual $R_{stem}$ between the two were slightly different (264 ± 88 and 191 ± 64 g C $m^{-2}$ $yr^{-1}$)
473 highlighting the possible variation of $R_{stem}$ for different trees. We did the measurement at a stem
474 height of 1.3 m. However, it has for some trees been found that stem $CO_2$ flux can vary with stem
475 height (Ceschia et al., 2002). This has been found to be caused by various amounts of $CO_2$

476 dissolved in the xylem that can diffuse out of the stem and therefore contribute to the apparent $CO_2$
477 flux measured by the chamber (Teskey and McGuire, 2002). Some of this $CO_2$ can be derived from
478 respiration produced elsewhere on the stem, or it can originate from $CO_2$ produced in the soil that is
479 being dissolved in the soil water, taken up by the roots and transported up through the stem (Aubrey
480 and Teskey, 2009; Bloemen et al., 2013; Teskey and Mcguire, 2007). Differences in $R_{stem}$ along the
481 height of the stems could potentially have influenced the annual estimate of $R_{stem}$, as well as
482 differences in $R_{stem}$ between different trees. This was, however, not tested in the current study.
483
484 **4.3 Different seasonal contribution of respiration components**
485 We found a strong seasonal pattern in the contributions of $R_{soil}$ and $R_{stem}$ to $R_{eco}$ (Fig. 2). $R_{eco}$
486 generally followed the variation in temperature throughout the year with highest $R_{eco}$ during the
487 summer growing season. This is usually seen for other temperate forest with growing season during
488 the warm and relatively wet summer (Janssens et al., 2000), in comparison to e.g. Mediterranean
489 ecosystems where $R_{eco}$ is decoupled from temperature during the hot and dry summers, when water
490 becomes a limiting factor (Matteucci et al., 2015).
491 The variation in the different seasonal contributions of the individual components to $R_{eco}$ have been
492 explained by differences in phenology, and their individual response to temperature (Migliavacca et
493 al., 2015). $R_{stem}$ experienced dramatic differences in the contribution to $R_{eco}$, with 6 % during winter
494 and 16 % during summer. Although following an overall pattern similar to $R_{soil}$ (Fig. 4), $R_{stem}$ was
495 much lower during winter. The deciduous beech trees shed their leaves during autumn and enter a
496 dormant period until spring. During this period they do not photosynthesize, and transpiration is
497 limited to a minimum (Essiamah and Eschrich, 1986). Thus the transport through the xylem and
498 phloem is limited to a minimum and respiration is limited to only the necessary maintenance
499 respiration (Damesin, 2003). However, during the growing season growth respiration may be a

500 significant part of stem respiration, not directly determined by temperature, but by plant phenology
501 (Lavigne and Ryan, 1997). The difference in $R_{stem}$ throughout the year may therefore be larger than
502 what can be expected from a general temperature dependence. Our observation of low $R_{stem}$, both in
503 absolute terms and in its contribution to $R_{eco}$ during the winter months, fits well with the pattern of
504 tree dormancy during winter, and increased growth respiration during summer. Similar seasonal
505 patterns of $R_{stem}$ have been found in other temperate forests (Acosta et al., 2008; Edwards et al.,
506 2002; Griffis et al., 2004; Shibistova et al., 2002; Yang et al., 2012, 2014). However, most studies
507 do not measure $R_{stem}$ during the winter months, making a full comparison difficult.
508 $R_{soil}$ from the manual chambers differed dramatically from $R_{stem}$ by showing a fairly similar
509 contribution to $R_{eco}$ during both winter, spring and summer of 52, 45 and 49 %, respectively, while
510 the contribution increased to 79 % during autumn. Unlike the trees, the microorganisms in the soil
511 do not go into dormancy and can continue to be active and respire, albeit at a slower rate, even
512 during winter (Beverly and Franklin, 2015). Freezing temperatures, which causes the soil to freeze
513 and lower $R_{soil}$ dramatically can occur at our site. However, the winter period during this study was
514 characterized by above-freezing temperatures during daytime for most of the winter; thereby
515 leaving the entire soil column thawed at most times. The very high contribution of $R_{soil}$ during
516 autumn coincided with leaf senescence and litterfall. The input of litter to the soil is significant at
517 the site, and has been found to account for 218 ± 17 g C $m^{-2}$ $yr^{-1}$ (Wu et al. 2013). Although the rate
518 of $R_{soil}$ is determined by temperature, the soil organisms will most often respond by increasing $R_{soil}$
519 if additional organic matter such as litter is put into the soil (Han et al., 2015). A continuous high
520 $R_{soil}$ or a peak following litterfall has been found for other temperate forest ecosystems (DeForest et
521 al., 2009; Hibbard et al., 2005). Thus, it is likely that the input of litter during autumn has kept $R_{soil}$
522 at our site high by fuelling heterotrophic respiration. The trees, however, have shed their leaves and
523 begun to enter dormancy, which lowers the relative contribution of plant respiration to $R_{eco}$.

524 The automated chamber measurements and the trenching revealed information on the contribution
525 of autotrophic $R_{soil}$ throughout the year. During summer, $R_{soil}$ of the trenched soil plots was only 51
526 % of $R_{soil}$ for the intact plots, while it increased to 83 % during autumn, which was comparable to
527 the pre trenching level of 77 %. This indicated that autotrophic $R_{soil}$ accounted for 49 % during
528 summer. However, before the trenching in April, $R_{soil}$ of the trenched plots was lower than the intact
529 soil plots, by only accounted for 77 %, thus indicating heterogeneous undisturbed $R_{soil}$. Accounting
530 for this pre trenching difference gives an autotrophic contribution of 34 % during summer.
531 The variation in the seasonal contribution of autotrophic $R_{soil}$ with highest contribution during the
532 plant growing season was expected and has been observed for several ecosystems (Beverly and
533 Franklin, 2015; Pumpanen et al., 2015; Hanson et al., 2000). The major reason for the seasonal
534 pattern of autotrophic $R_{soil}$ is the seasonal pattern of GPP that drives an increase in root respiration
535 during the growing season (Pumpanen et al., 2015). Hanson et al. (2000) reviewed the contribution
536 of autotrophic $R_{soil}$ for different ecosystems and found that the contribution of autotrophic
537 respiration varied from 10 % to more than 90 %, with a mean value for forests of 45.8 %. 50 %
538 autotrophic $R_{soil}$ was found in a mixed beech spruce forest in the south of Germany (Andersen et al.,
539 2005). Epron et al., (2001) found a mean autotrophic $R_{soil}$ of 52 %, with highest autotrophic rate of
540 60 % in July in a French beech forest. Brumme (1995) found that autotrophic respiration comprised
541 40 % in a central German beech forest. Our trenching was performed in April, making a full
542 comparison for the entire year impossible. Our estimate of an autotrophic contribution of 34 %
543 during summer is relatively low compared to prior literature values. However, since the trenching
544 was only performed a few months prior to the measurements, it is possible that decomposing root
545 litter from the severed roots may have contributed to the trenched plots, thereby leading to an
546 overestimated heterotrophic $R_{soil}$ (Díaz-Pinés et al., 2010; Epron et al., 1999; Hanson et al., 2000;

547 Silver et al., 2005; Subke et al., 2006). A second possibility is the presence of deeper living roots
548 below the trenching depth of 25 cm.
549 Instead of following the variation in GPP, $R_{stem}$ more closely followed $R_{soil}$ and temperature during
550 spring, summer and autumn (Fig. 4, Fig. 3). Thus the high variation in GPP during the growing
551 season was not seen for $R_{stem}$, which could indicate that the magnitude of $R_{stem}$ was independent
552 from the day to day variations in GPP and the associated high respiration rates that are expected for
553 the photosynthesizing organs. The dependence on temperature is in line with other studies that have
554 found a clear temperature dependence of $R_{stem}$ (Harris et al., 2008; Lavigne et al., 1996; Ryan et al.,
555 1995), although photosynthesis has also been found to partially regulate stem respiration (Zha et al.,
556 2004).
557
558 **4.4 Diel patterns of respiration**
559 Both $R_{stem}$ and $R_{root}$ showed a clear diel pattern during summer with the highest respiration seen
560 around 13:00-15:00 CET for $R_{stem}$, and the highest respiration seen from 9:00-15:00 for $R_{root}$ (Fig.
561 5o, k). The high $R_{stem}$ during the afternoon is consistent with the findings of other studies (Acosta et
562 al., 2008; Teskey and Mcguire, 2007; Zha et al., 2004). This distinct diel pattern have been
563 explained by a temperature response to the diel pattern of temperature (Teskey and Mcguire, 2007).
564 However, other studies have found diel patterns of $R_{stem}$ different from the diel pattern of
565 temperature, which has been suggested to be due to the diel pattern of $R_{stem}$ being modified by
566 photosynthesis and cambium activity independent of temperature (Yang et al., 2014). The diel
567 pattern of $R_{stem}$ during summer in our study followed the diel pattern of air temperature, thus
568 suggesting that temperature is a main determining factor for $R_{stem}$ at our site. This is in line with
569 temperature being the determining factor for $R_{stem}$ at the seasonal scale (Fig. 4, Section 4.3).
570 However, during winter $R_{stem}$ was very low and showed no diel pattern, which could reflect the tree

571 dormancy during this period (Fig. 5m). The high $R_{root}$ during 9:00-15:00 is consistent with the
572 findings of other studies that saw highest $R_{root}$ during daytime, which often has been found to be
573 linked with photosynthesis (Chen et al., 2010; Drake et al., 2008; Lai et al., 2016; Wertin and
574 Teskey, 2008). During daytime, an increase in $R_{root}$ is seen due to respiration of recently fixed
575 photosynthates. During nighttime, however, no photosynthesis takes place, leading to the diel
576 pattern in feeding of photosynthates. Photosynthesis at the DK-Sor site usually peaks at noon,
577 before the peak in temperature (Pilegaard et al., 2001). This is consistent with the peak in $R_{root}$ in
578 this study, thus indicating that photosynthates might in part determine the diel pattern of $R_{root}$ during
579 summer. Interestingly, no diel pattern was seen during winter and autumn (Fig. 5i, l). During
580 winter, no photosynthesis takes place, and only little photosynthesis takes place in autumn, thus
581 only a small amount of photosynthates can alter the diel pattern during these periods. During spring,
582 however, a small peak was seen around 15:00 CET, later than the peak seen during summer (Fig.
583 5j). Spring was the only season that showed a diel pattern of soil temperature at 5 cm depth (Fig.
584 6b). Thus, it is possible that the temperature response of $R_{root}$ is dominant during spring.
585 No clear difference in the diel pattern of $R_{soil}$ was seen between the intact and trenched soil plots
586 (Fig. 5a-h). However, the trenched plots had lower $R_{soil}$ following the trenching, indicating that the
587 autotrophic contribution to $R_{soil}$ had been completely or partly removed from the trenched plots
588 (Section 4.3). Heterotrophic $R_{soil}$ has generally been found to respond to temperature on a seasonal
589 scale, as well as on a diel scale, although a hysteresis on the diel scale between soil temperature and
590 heterotrophic $R_{soil}$ has also been observed (Chen et al., 2009; Song et al., 2015; Zhang et al., 2015).
591 In contrast, autotrophic $R_{soil}$ has often been found to be decoupled from temperature on a diel scale,
592 resulting primarily from substrate transfer to the soil bacteria through carbon exudates from plant
593 roots (Kuzyakov and Gavrichkova, 2010). Similarly to the increase in $R_{root}$ as a result of increased
594 levels of fresh photosynthates, the increase in $R_{soil}$ has been found to lag after photosynthesis

595 (Savage et al., 2013; Tang et al., 2005). Whereas we saw an increase in $R_{root}$ during daytime, we did
596 not see a similar increase in $R_{soil}$ during daytime in the intact soil plot that contained roots. Instead,
597 a lower daytime $R_{soil}$ was seen for both the intact and trenched soil plots. Soil temperature at 5 cm
598 depth generally showed no diel pattern for winter, summer and autumn, which would mean no diel
599 pattern in $R_{soil}$ if only determined by temperature (Fig. 6). It was surprising that no difference was
600 seen between the intact and trenched soil plots. In a previous study at the site, the diel pattern of
601 $R_{soil}$ was investigated for intact soil (Brændholt et al. 2017). A similar diel pattern with lower
602 daytime $R_{soil}$ was observed. However, it was found that the measured soil $CO_2$ fluxes were
603 influenced by low atmospheric turbulence, which was found to lead to an overestimation of
604 measured soil $CO_2$ fluxes especially during nighttime, which in turn also biased the diel pattern. In
605 the current study, we removed measurements at low atmospheric turbulence to remove the effect of
606 overestimation of fluxes, as recommended by Brændholt et al. (2017). It is, however, possible that
607 overestimation still plays a role. If this effect is larger than the potential differences in the diel
608 patterns of intact soil and trenched soil, then this effect may overrule the real diel patterns, making
609 it difficult to make a distinction between the diel patterns.
610

611 # 5 Conclusions

612 In this study we used the eddy covariance technique together with manual and automated closed-
613 chambers to quantify the individual components of ecosystem respiration at diel, seasonal and
614 annual scale. We found that the contribution of $R_{stem}$ to total $R_{eco}$ varied throughout the year, by only
615 accounting for 6 % of $R_{eco}$ during winter and 16 % during the summer growing season. In contrast,
616 $R_{soil}$ showed a fairly similar contribution to $R_{eco}$ during winter, spring and summer of 52, 45 and 49
617 %, respectively, while the contribution increased to 79 % during autumn. We attributed the large
618 difference in the seasonal contribution of $R_{stem}$ to different phenological stages of dormancy and

growth experienced for the trees during the year, whereas we attributed the high contribution of $R_{soil}$ in autumn to the large input of litter from the deciduous beech trees.

By the trenching method, we partitioned $R_{soil}$ into its heterotrophic and autotrophic components. We found that autotrophic $R_{soil}$ accounted for 34 % of $R_{soil}$ during summer, a relative low value compared to findings from other studies. However, we could not rule out the possibility that decomposing roots from the trenched soil plots might have led to an overestimated heterotrophic $R_{soil}$.

Diel $R_{stem}$ and $R_{root}$ showed a clear pattern during summer with the highest respiration seen around 13:00-15:00 CET for $R_{stem}$, and the highest respiration seen from 9:00-15:00 for $R_{root}$. In contrast, $R_{soil}$ showed the lowest respiration during daytime $R_{soil}$ with no clear difference in the diel pattern between the intact and trenched soil plots.

Finally, we calculated annual $R_{soil}$ for different transects at the site, and found that annual $R_{soil}$ estimated from the previously used transect at the site was underestimated due to $R_{soil}$ of the transect not being representative for the spatial heterogeneity of $R_{soil}$ at the site. This highlighted the importance of performing a sufficient number of manual chamber measurements at a site to adequately capture the spatial variation in $R_{soil}$, and thereby to correctly estimate $R_{soil}$.

# Acknowledgements

This study was funded by the Danish Ministry for Research, Innovation and Higher Education, the Danish Council for Independent Research (DFF – 1323-00182).

# References


Acosta, M., Pavelka, M., Pokorný, R., Janouš, D., Marek, M.V., 2008. Seasonal variation in $CO_2$ efflux of stems and branches of Norway spruce trees. Ann. Bot. 101, 469–477.

Andersen, C.P., Nikolov, I., Nikolova, P., Matyssek, R., Häberle, K.H., 2005. Estimating "autotrophic" belowground respiration in spruce and beech forests: Decreases following girdling. Eur. J. For. Res. 124, 155–163.

Aubrey, D.P., Teskey, R.O., 2009. Root-derived $CO_2$ efflux via xylem stream rivals soil $CO_2$ efflux. New Phytol. 184, 35–40.

Baggs, E.M., 2006. Partitioning the components of soil respiration: A research challenge. Plant Soil. 284, 1–5.

Beer, C., Reichstein, M., Tomelleri, E., Ciais, P., Jung, M., Carvalhais, N., Rödenbeck, C., Arain, M.A., Baldocchi, D., Bonan, G.B., Bondeau, A., Cescatti, A., Lasslop, G., Lindroth, A., Lomas, M., Luyssaert, S., Margolis, H., Oleson, K.W., Roupsard, O., Veenendaal, E., Viovy, N., Williams, C., Woodward, F.I., Papale, D., 2010. Terrestrial gross carbon dioxide uptake: Global distribution and covariation with climate. Science. 329, 834-838.

Beverly, D., Franklin, S., 2015. Heterotrophic and Autotrophic Soil Respiration under Simulated Dormancy Conditions. Open J. For. 5, 274–286.

Bloemen, J., Mcguire, M.A., Aubrey, D.P., Teskey, R.O., Steppe, K., 2013. Transport of root-respired $CO_2$ via the transpiration stream affects aboveground carbon assimilation and $CO_2$ efflux in trees. New Phytol. 197, 555–565.

Bond-Lamberty, B., Bronson, D., Bladyka, E., Gower, S.T., 2011. A comparison of trenched plot techniques for partitioning soil respiration. Soil Biol. Biochem. 43, 2108–2114.

Brændholt, A., Larsen, K.S., Ibrom, A., Pilegaard, K., 2017. Overestimation of closed-chamber soil $CO_2$ effluxes at low atmospheric turbulence. Biogeosciences. 14, 1603-1616.

664 Brumme, R., 1995. Mechanisms of carbon and nutrient release and retention in beech forest gaps.
665 Plant Soil. 168-169, 593–600.
666 Ceschia, É., Damesin, C., Lebaube, S., Pontailler, J.Y., Dufrêne, É., 2002. Spatial and seasonal
667 variations in stem respiration of beech trees (*Fagus sylvatica*). Ann. For. Sci. 59, 801–812.
668 Chen, D., Zhou, L., Rao, X., Lin, Y., Fu, S., 2010. Effects of root diameter and root nitrogen
669 concentration on in situ root respiration among different seasons and tree species. Ecol. Res.
670 25, 983–993.
671 Chen, J.M., Huang, S.E., Ju, W., Gaumont-Guay, D., Black, T.A., 2009. Daily heterotrophic
672 respiration model considering the diurnal temperature variability in the soil. J. Geophys. Res.
673 114, G01022, 1-11.
674 Ciais, P., Reichstein, M., Viovy, N., Granier, A., Ogée, J., Allard, V., Aubinet, M., Buchmann, N.,
675 Bernhofer, C., Carrara, A., Chevallier, F., De Noblet, N., Friend, A.D., Friedlingstein, P.,
676 Grünwald, T., Heinesch, B., Keronen, P., Knohl, A., Krinner, G., Loustau, D., Manca, G.,
677 Matteucci, G., Miglietta, F., Ourcival, J.M., Papale, D., Pilegaard, K., Rambal, S., Seufert, G.,
678 Soussana, J.F., Sanz, M.J., Schulze, E.D., Vesala, T., Valentini, R., 2005. Europe-wide
679 reduction in primary productivity caused by the heat and drought in 2003. Nature. 437, 529–
680 533.
681 Damesin, C., 2003. Respiration and photosynthesis characteristics of current-year stems of Fagus
682 sylvatica: From the seasonal pattern to an annual balance. New Phytol. 158, 465–475.
683 Damesin, C., Ceschia, E., Le Goff, N., Ottorini, J.M., Dufrene, E. 2002. Stem and branch
684 respiration of beech: from tree measurements to estimations at the stand level. New Phytol.
685 153, 159–172.
686 Davidson, E.A., Savage, K., Verchot, L.V., Navarro, R., 2002. Minimizing artifacts and biases in
687 chamber-based measurements of soil respiration. Agric. For. Meteorol. 113, 21–37.

688 DeForest, J.L., Chen, J., McNulty, S.G., 2009. Leaf litter is an important mediator of soil respiration
689 in an oak-dominated forest. Int. J. Biometeorol. 53, 127–134.
690 Department of Biogeochemical Integration, MPI Jena, 2017. REddyProc: Eddy covariance data
691 processing tool. http://www.bgc-jena.mpg.de/REddyProc/brew/REddyProc.rhtml (accessed
692 17.05.29).
693 Díaz-Pinés, E., Schindlbacher, A., Pfever, M., Jandl, R., Zechmeister-Boltenstern, S., Rubio, A.,
694 2010. Root trenching: A useful tool to estimate autotrophic soil respiration? A case study in an
695 austrian mountain forest. Eur. J. For. Res. 129, 101–109.
696 Drake, J.E., Stoy, P.C., Jackson, R.B., DeLucia, E.H., 2008. Fine-root respiration in a loblolly pine
697 (*Pinus taeda* L.) forest exposed to elevated $CO_2$ and N fertilization. Plant, Cell Environ. 31,
698 1663–1672.
699 Edwards, N.T., Hanson, P.J., 1996. Stem respiration in a closed-canopy upland oak forest. Tree
700 Physiol. 16, 433–439.
701 Edwards, N.T., Tschaplinski, T.J., Norby, R.J., 2002. Stem respiration increases in $CO_2$-enriched
702 sweetgum trees. New Phytol. 155, 239–248.
703 Elzhov, V.T., Mullen, K.M., Spiess, A., Bolker, B., 2016. minpack.lm: R Interface to the
704 Levenberg-Marquardt Nonlinear Least-Squares Algorithm Found in MINPACK, Plus Support
705 for Bounds, R package version 1.2-0. http://CRAN.R-project.org/package=minpack.lm
706 (accessed 17.05.29).
707 Epron, D., Farque, L., Lucot, E., Badot, P.M., 1999. Efflux in a Beech Forest: the Contribution of
708 Root Respiration. Ann. For. Sci. 56, 289–295.
709 Epron, D., Le Dantec, V., Dufrene, E., Granier, A., 2001. Seasonal dynamics of soil carbon dioxide
710 efflux and simulated rhizosphere respiration in a beech forest. Tree Physiol. 21, 145–152.

711 Essiamah, S., Eschrich, W., 1986. Water Uptake in Deciduous Trees During Winter and the Role of
712 Conducting Tissues in Spring Reactivation. IAWA Journal. 7, 31-38.
713 Griffis, T.J., Black, T.A., Gaumont-Guay, D., Drewitt, G.B., Nesic, Z., Barr, A.G., Morgenstern,
714 K., Kljun, N., 2004. Seasonal variation and partitioning of ecosystem respiration in a southern
715 boreal aspen forest. Agric. For. Meteorol. 125, 207–223.
716 Hanson, P.J., Edwards, N.T., Garten, C.T., Andrews, J.A., 2000. Separating root and soil microbial
717 contributions to soil respiration: A review of methods and observations. Biogeochemistry. 48,
718 115–146.
719 Han, T., Huang, W., Liu, J., Zhou, G., Xiao, Y., 2015. Different soil respiration responses to litter
720 manipulation in three subtropical successional forests. Sci. Rep. 5, 18166.
721 Harris, N.L., Hall, C.A.S., Lugo, A.E., 2008. Estimates of species- and ecosystem-level respiration
722 of woody stems along an elevational gradient in the Luquillo Mountains, Puerto Rico. Ecol.
723 Modell. 216, 253–264.
724 Hibbard, K.A., Law, B.E., Reichstein, M., Sulzman, J., 2005. An analysis of soil respiration across
725 northern hemisphere temperate ecosystems. Biogeochemistry. 73, 29–70.
726 Högberg, P., Nordgren, A., Högberg, M.N., Ottosson-Lofvenius, M., Bhupinderpal, S., Olsson, P.,
727 Linder, S., 2005. Fractional contributions by autotrophic and heterotrophic respiration to soil-
728 surface $CO_2$ efflux in boreal forests. SEB Exp Biol Ser. 251–267.
729 Hutchinson, G.L., Mosier, A.R., 1981. Improved soil cover method for field measurement of
730 nitrous oxide fluxes. Soil Sci. Soc. Am. J. 45, 311–316.
731 Ibrom, A., Jarvis, P.G., Clement, R.B., Morgenstern, K., Oltchev, A., Medlyn, B., Wang, Y.P.,
732 Wingate, L., Moncrieff, J., Gravenhorst, G., 2006. A comparative analysis of simulated and
733 observed photosynthetic $CO_2$ uptake in two coniferous forest canopies. Tree Physiol. 26, 845–
734 864.

735 Inoue, A., 2004. Relationships of stem surface area to other stem dimensions for Japanese cedar
736 (*Cryptomeria japonica* D. Don) and Japanese cypress (*Chamaecyparis obtusa* Endl.) trees. J.
737 For. Res. 9, 45–50.
738 IPCC, 2013. Climate Change 2013: the Physical Science Basis. Contribution of Working Group I to
739 the Fifth Assessment Report of the Intergovernmental Panel on Climate Change. Cambridge
740 University Press, Cambridge, United Kingdom and New York, NY, USA. 1535.
741 Janssens, I., Pilegard, K., 2003. Large seasonal changes in $Q_{10}$ of soil respiration in a beech forest.
742 Global Biogeochem. Cycles. 9, 911–918.
743 Janssens, I.A., Lankreijer, H., Matteucci, G., Kowalski, A.S., Buchmann, N., Epron, D., Pilegaard,
744 K., Kutsch, W., Longdoz, B., Grünwald, T., Montagnani, L., Dore, S., Rebmann, C., Moors, E.
745 J., Grelle, A., Rannik, Ü., Morgenstern, K., Oltchev, S., Clement, R., Gudmundsson, J.,
746 Minerbi, S., Berbigier, P., Ibrom, A., Moncrieff, J., Aubinet, M., Bernhofer, C., Jensen, N.O.,
747 Vesala, T., Granier, A., Schulze, E.D., Lindroth, A., Dolman, A.J., Jarvis, P.G., Ceulemans, R.,
748 Valentini, R., 2000. Productivity overshadows temperature in determining soil and ecosystem
749 respiration across European forests. Glob. Chang. Biol. 7, 269–278.
750 Knohl, A., Søe, A.R.B., Kutsch, W.L., Göckede, M., Buchmann, N., 2008. Representative estimates
751 of soil and ecosystem respiration in an old beech forest. Plant Soil. 302, 189–202.
752 Kuzyakov, Y., Gavrichkova, O., 2010. Time lag between photosynthesis and carbon dioxide efflux
753 from soil: A review of mechanisms and controls. Glob. Chang. Biol. 16, 3386–3406.
754 Lai, Z., Lu, S., Zhang, Y., Wu, B., Qin, S., Feng, W., Liu, J., Fa, K., 2016. Diel patterns of fine root
755 respiration in a dryland shrub, measured in situ over different phenological stages. J. For. Res.
756 21, 31–42.
757 Landesverwaltungsamt Sachsen-Anhalt, 2011. Leitfaden zur Vorratsermittlung von Waldbeständen
758 und zur Bewertung forstrechtlicher Sachverhalte (In german). https://lvwa.sachsen-

759 anhalt.de/fileadmin/Bibliothek/Politik_und_Verwaltung/LVWA/LVwA/Dokumente/pressestell
760 e/publikationen/broschueren/vorratsermittlung.pdf (accessed 17.05.29).
761 Lasslop, G., Reichstein, M., Papale, D., Richardson, A., Arneth, A., Barr, A., Stoy, P., Wohlfahrt,
762 G., 2010. Separation of net ecosystem exchange into assimilation and respiration using a light
763 response curve approach: critical issues and global evaluation. Glob. Chang. Biol. 16, 187-208.
764 Lavigne, M.B., Franklin, S.E., Hunt Jr, E.R., 1996. Estimating stem maintenance respiration rates
765 of dissimilar balsam fir stands. Tree Physiol. 16, 687–95.
766 Lavigne, M.B., Ryan, M.G., 1997. Growth and maintenance respiration rates of aspen, black spruce
767 and jack pine stems at northern and southern BOREAS sites. Tree Physiol. 17, 543–551.
768 Lloyd, J., Taylor, J.A., 1994. On the temperature dependence of soil respiration. Funct. Ecol. 8,
769 315–323.
770 Luyssaert, S., Inglima, I., Jung, M., Richardson, A.D., Reichstein, M., Papale, D., Piao, S.L.,
771 Schulze, E.D., Wingate, L., Matteucci, G., Aragao, L., Aubinet, M., Beer, C., Bernhofer, C.,
772 Black, K.G., Bonal, D., Bonnefond, J.M., Chambers, J., Ciais, P., Cook, B., Davis, K.J.,
773 Dolman, A.J., Gielen, B., Goulden, M., Grace, J., Granier, A., Grelle, A., Griffis, T.,
774 Grünwald, T., Guidolotti, G., Hanson, P.J., Harding, R., Hollinger, D.Y., Hutyra, L.R., Kolari,
775 P., Kruijt, B., Kutsch, W., Lagergren, F., Laurila, T., Law, B.E., Le Maire, G., Lindroth, A.,
776 Loustau, D., Malhi, Y., Mateus, J., Migliavacca, M., Misson, L., Montagnani, L., Moncrieff,
777 J., Moors, E., Munger, J.W., Nikinmaa, E., Ollinger, S.V., Pita, G., Rebmann, C., Roupsard,
778 O., Saigusa, N., Sanz, M.J., Seufert, G., Sierra, C., Smith, M.L., Tang, J., Valentini, R., Vesala,
779 T., Janssens, I.A., 2007. $CO_2$ balance of boreal, temperate, and tropical forests derived from a
780 global database. Glob. Chang. Biol. 13, 2509–2537.
781 Mahecha, M.D., Reichstein, M., Carvalhais, N., Lasslop, G., Lange, H., Seneviratne, S.I., Vargas,
782 R., Ammann, C., Arain, M.A., Cescatti, A., Janssens, I.A., Migliavacca, M., Montagnani, L.,

783 Richardson, A.D., 2010. Global Convergence in the Temperature Sensitivity of Respiration at
784 Ecosystem Level, Science. 329, 838–840.
785 Matteucci, M., Gruening, C., Goded Ballarin, I., Seufert, G., Cescatti, A., 2015. Components,
786 drivers and temporal dynamics of ecosystem respiration in a Mediterranean pine forest. Soil
787 Biol. Biochem. 88, 224–235.
788 Migliavacca, M., Reichstein, M., Richardson, A.D., Mahecha, M.D., Cremonese, E., Delpierre, N.,
789 Galvagno, M., Law, B.E., Wohlfahrt, G., Andrew Black, T., Carvalhais, N., Ceccherini, G.,
790 Chen, J., Gobron, N., Koffi, E., William Munger, J., Perez-Priego, O., Robustelli, M.,
791 Tomelleri, E., Cescatti, A., 2015. Influence of physiological phenology on the seasonal pattern
792 of ecosystem respiration in deciduous forests. Glob. Chang. Biol. 21, 363–376.
793 Nagy, M.T., Janssens, I.A., Curiel Yuste, J., Carrara, A., Ceulemans, R., 2006. Footprint-adjusted
794 net ecosystem $CO_2$ exchange and carbon balance components of a temperate forest. Agric. For.
795 Meteorol. 139, 344–360.
796 Østergård, J., 2000. Jordbundsdannelse under bøgeskov og mark ved Lille Bøgeskov, Sorø.
797 Master's thesis, Department of Earth Sciences, University of Aarhus, Denmark, (in Danish).
798 Peichl, M., Sonnentag, O., Wohlfahrt G., Flanagan, L.B., Baldocchi, D.D., Kiely, G., Galvagno, M.,
799 Gianelle, D., Marcolla, B., Pio, C., Migliavacca, M., Jones, M.B., Saunders, M., 2013.
800 Convergence of potential net ecosystem production among contrasting $C_3$ grasslands. Ecology
801 Letters. 16, 502–512.
802 Pilegaard, K., Hummelshøj, P., Jensen, N.O., Chen, Z., 2001. Two years of continuous $CO_2$ eddy-
803 flux measurements over a Danish beech forest. 107, 29–41.
804 Pilegaard, K., Ibrom, A., Courtney, M.S., Hummelshøj, P., Jensen, N.O., 2011. Increasing net $CO_2$
805 uptake by a Danish beech forest during the period from 1996 to 2009. Agric. For. Meteorol.
806 151, 934–946.

807 Pumpanen, J., Kulmala, L., Lindén, A., Kolari, P., Nikinmaa, E., 2015. Seasonal dynamics of
808 autotrophic respiration in boreal forest soil estimated by continuous chamber measurements.
809 Boreal Environ. Res. 20, 637–650.
810 R Core Team, 2014. R: A language and environment for statistical computing. R Foundation for
811 Statistical Computing, Vienna, Austria.
812 Reichstein, M., Falge, E., Baldocchi, D., Papale, D., Aubinet, M., Berbigier, P., Bernhofer, C.,
813 Buchmann, N., Gilmanov, T., Granier, A., Grünwald, T., Havránková, K., Ilvesniemi, H.,
814 Janous, D., Knohl, A., Laurila, T., Lohila, A., Loustau, D., Matteucci, G., Meyers, T.,
815 Miglietta, F., Ourcival, J.M., Pumpanen, J., Rambal, S., Rotenberg, E., Sanz, M., Tenhunen, J.,
816 Seufert, G., Vaccari, F., Vesala, T., Yakir, D., Valentini, R., 2005. On the separation of net
817 ecosystem exchange into assimilation and ecosystem respiration: Review and improved
818 algorithm. Glob. Chang. Biol. 11, 1424–1439.
819 Rodeghiero, M., Cescatti, A., 2006. Indirect partitioning of soil respiration in a series of evergreen
820 forest ecosystems. Plant Soil. 284, 7–22.
821 Rodríguez-Calcerrada, J., Martin-StPaul, N.K., Lempereur, M., Ourcival, J.M., Rey, M. del C. del,
822 Joffre, R., Rambal, S., 2014. Stem $CO_2$ efflux and its contribution to ecosystem $CO_2$ efflux
823 decrease with drought in a Mediterranean forest stand. Agric. For. Meteorol. 195–196, 61–72.
824 Ryan, M.G., Gower, S.T., Hubbard, R.M., Waring, R.H., Gholz, H.L., Cropper, W.P., Running,
825 S.W., 1995. Woody tissue maintenance respiration of four conifers in contrasting climates.
826 Oecologia. 101, 133–140.
827 Savage, K., Davidson, E.A., Richardson, D.A., 2008. A conceptual and practical approach to data
828 quality and analysis procedures for high-frequency soil respiration measurements. Funct. Ecol.
829 22, 1000–1007.

Savage, K., Davidson, E.A., Tang, J., 2013. Diel patterns of autotrophic and heterotrophic respiration among phenological stages. Glob. Chang. Biol. 19, 1151–1159.

Savage, K.E., Davidson, E.A., 2003. A comparison of manual and automated systems for soil $CO_2$ flux measurements: Trade-offs between spatial and temporal resolution. J. Exp. Bot. 54, 891–899.

Saveyn, A., Steppe, K., Lemeur, R., 2007. Daytime depression in tree stem $CO_2$ efflux rates: Is it caused by low stem turgor pressure? Ann. Bot. 99, 477–485.

Schimel, D.S., House, J.I., Hibbard, K.A, Bousquet, P., Ciais, P., Peylin, P., Braswell, B.H., Apps, M.J., Baker, D., Bondeau, A, Canadell, J., Churkina, G., Cramer, W., Denning, A.S., Field, C.B., Friedlingstein, P., Goodale, C., Heimann, M., Houghton, R.A., Melillo, J.M., Moore, B., Murdiyarso, D., Noble, I., Pacala, S.W., Prentice, I.C., Raupach, M.R., Rayner, P.J., Scholes, R.J., Steffen, W.L., Wirth, C., 2001. Recent patterns and mechanisms of carbon exchange by terrestrial ecosystems. Nature. 414, 169–172.

Shibistova, O., Lloyd, J., Zrazhevskaya, G., Arneth, A., Kolle, O., Knohl, A., Astrakhantceva, N., Shijneva, I., Schmerler, J., 2002. Annual ecosystem respiration budget for a *Pinus sylvestris* stand in central Siberia. Tellus. 54B, 568–589.

Silver, W.L., Thompson, A.W., McGroddy, M.E., Varner, R.K., Dias, J.D., Silva, H., Crill, P.M., Keller, M., 2005. Fine root dynamics and trace gas fluxes in two lowland tropical forest soils. Glob. Chang. Biol. 11, 290–306.

Song, W., Chen, S., Zhou, Y., Wu, B., Zhu, Y., Lu, Q., Lin, G., 2015. Contrasting diel hysteresis between soil autotrophic and heterotrophic respiration in a desert ecosystem under different rainfall scenarios. Sci Rep. 5, 16779.

Subke, J.A., Inglima, I., Cotrufo, M.F., 2006. Trends and methodological impacts in soil $CO_2$ efflux partitioning: A metaanalytical review. Glob. Chang. Biol. 12, 921–943.

854 Tang, J., Baldocchi, D.D., Xu, L., 2005. Tree photosynthesis modulates soil respiration on a diurnal
855 time scale. Glob. Chang. Biol. 11, 1298–1304.
856 Tang, J., Bolstad, P.V., Desai, A.R., Martin, J.G., Cook, B.D., Davis, K.J., Carey, E.V., 2008.
857 Ecosystem respiration and its components in an old-growth forest in the Great Lakes region of
858 the United States. Agric. For. Meteorol. 148, 171–185.
859 Teskey, R.O., McGuire, M.A., 2002. Carbon dioxide transport in xylem causes errors in estimation
860 of rates of respiration in stems and branches of trees. Plant, Cell Environ. 25, 1571–1577.
861 Teskey, R.O., Mcguire, M.A., 2007. Measurement of stem respiration of sycamore (*Platanus*
862 *occidentalis* L.) trees involves internal and external fluxes of $CO_2$ and possible transport of
863 $CO_2$ from roots. Plant, Cell Environ. 30, 570–579.
864 Valentini, R., Matteucci, G., Dolman, A.J., Schulze, E.D., Jarvis, P.G., 2003. The carbon sink
865 strength of forests in Europe: a synthesis of results. In: Valentini, R. (Ed.), Fluxes of Carbon,
866 Water and Energy of European Forests, Ecological Studies, vol. 163. Springer, Berlin.
867 Van Oijen, M., Rougier, J., Smith, R., 2005. Bayesian calibration of process-based forest models:
868 bridging the gap between models and data. Tree Physiol. 25 (7), 915–927.
869 Wang, M., Guan, D.X., Han, S.J., Wu, J.L., 2010. Comparison of eddy covariance and chamber-
870 based methods for measuring $CO_2$ flux in a temperate mixed forest. Tree Physiol. 30, 149–163.
871 Webster, K.L., Creed, I.F., Bourbonnière, R.A., Beall, F.D., 2008. Controls on the heterogeneity of
872 soil respiration in a tolerant hardwood forest. J. Geophys. Res. Biogeosciences 113, 1–15.
873 Wertin, T.M., Teskey, R.O., 2008. Close coupling of whole-plant respiration to net photosynthesis
874 and carbohydrates. Tree Physiol. 28, 1831–40.
875 Wofsy, S.C., Goulden, M.L., Munger, J.W., Fan, S.M., Bakwin, P.S., Daube, B.C., Bassow, S.L.,
876 Bazzaz, F.A., 1993. Net exchange of $CO_2$ in a mid-latitude forest. Science. 260, 1314 – 1317.

877 Wu, J., Larsen, K.S., van der Linden, L., Beier, C., Pilegaard, K., Ibrom, A., 2013. Synthesis on the
878 carbon budget and cycling in a Danish, temperate deciduous forest. Agric. For. Meteorol. 181,
879 94–107.
880 Yang, J., He, Y., Aubrey, D.P., Zhuang, Q., Teskey, R.O., 2015. Global patterns and predictors of
881 stem $CO_2$ efflux in forest ecosystems. Glob. Chang. Biol. 22, 1433–1444.
882 Yang, J.Y., Teskey, R.O., Wang, C.K., 2012. Stem $CO_2$ efflux of ten species in temperate forests in
883 Northeastern China. Trees - Struct. Funct. 26, 1225–1235.
884 Yang, Y., Zhao, M., Xu, X., Sun, Z., Yin, G., Piao, S., 2014. Diurnal and seasonal change in stem
885 respiration of Larix principis-rupprechtii trees, northern China. PLoS One. 9, 1–7.
886 Zha, T., Kellomäki, S., Wang, K.Y., Ryyppö, A., Niinistö, S., 2004. Seasonal and annual stem
887 respiration of scots pine trees under boreal conditions. Ann. Bot. 94, 889–896.
888 Zhang, Q., Katul, G.G., Oren, R., Daly, E., Manzoni, S., Yang, D., Al, Z.E.T., 2015. The hysteresis
889 response of soil $CO_2$ concentration and soil respiration to soil temperature. J. Geophys. Res.
890 Biogeosci. 120, 1605–1618.
891 Zhu, L.W., Zhao, P., Ni, G.Y., Cao, Q.P., Zhou, C.M., Zeng, X.P., 2012. Individual-and stand-level
892 stem $CO_2$ efflux in a subtropical *Schima superba* plantation. Biogeosciences. 9, 3729–3737.
893

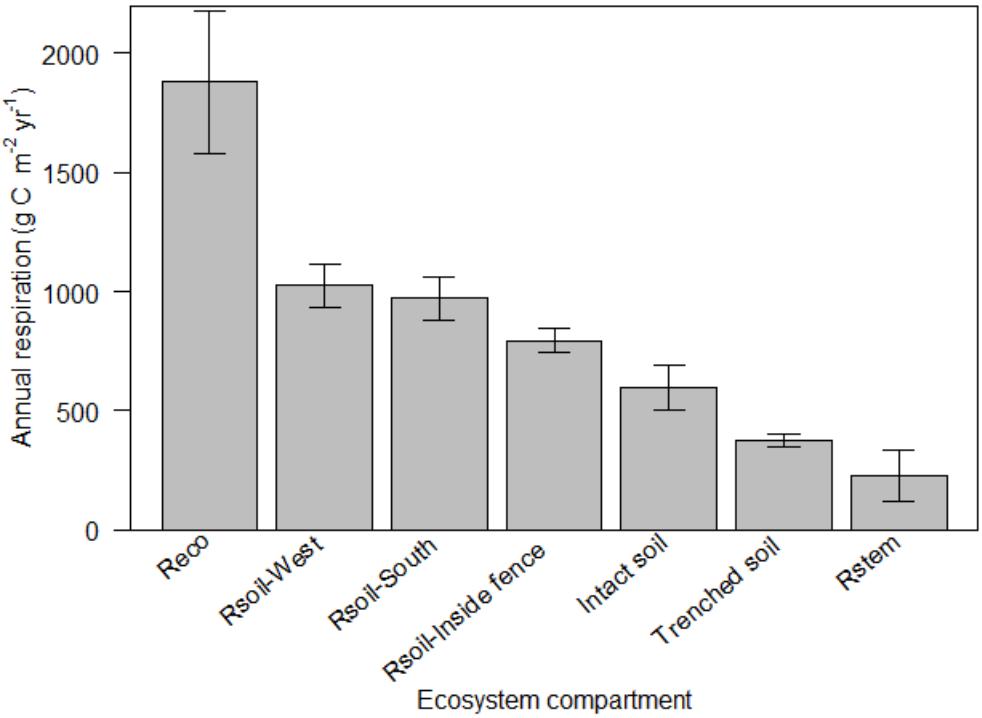


894

895 **Figure 1:** Annual respiration for the different components of the ecosystem, with the estimated
896 uncertainties shown by error bars. From left to right the bars show: $R_{eco,}$ $R_{soil}$ at the west transect,
897 $R_{soil}$ at the south transect, $R_{soil}$ at the inside fence transect, $R_{soil}$ at the intact soil plots measured by
898 the automated chambers, $R_{soil}$ at the trenched soil plots measured by the automated chambers and
899 $R_{stem}$. The annual estimated GPP was 2272 ± 136 g C $m^{-2}$ $yr^{-1}$.

900

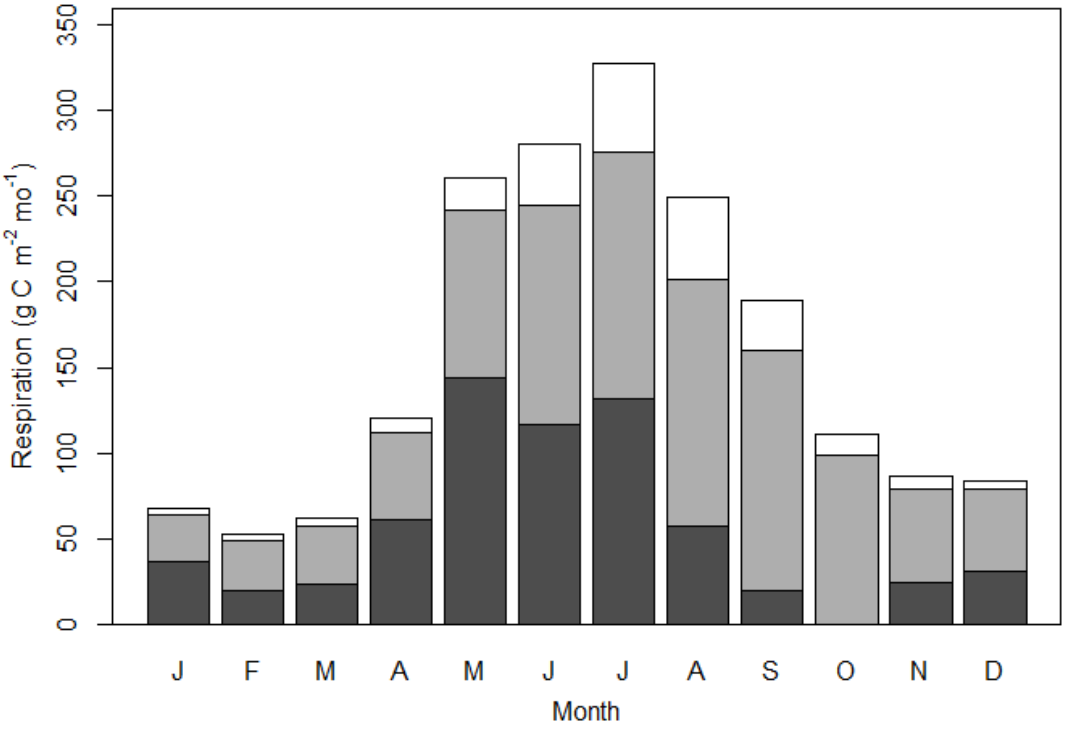


**Figure 2:** $R_{eco}$ (total bar height) partitioned into the component respiration rates from $R_{soil}$ (grey) and $R_{stem}$ (white) on a surface area basis for each month of 2016. The black bars represent the remaining $R_{eco}$ after $R_{soil}$ and $R_{stem}$ have been subtracted, i.e. from tree branches and leaves. For the monthly $R_{soil}$, the average of the manual closed-chamber measurements of the south and west transect is shown. Note, that for October, $R_{eco}$ was 11.9 g C $m^{-2}$ $yr^{-1}$ lower than the sum of $R_{stem}$ and $R_{soil}$.

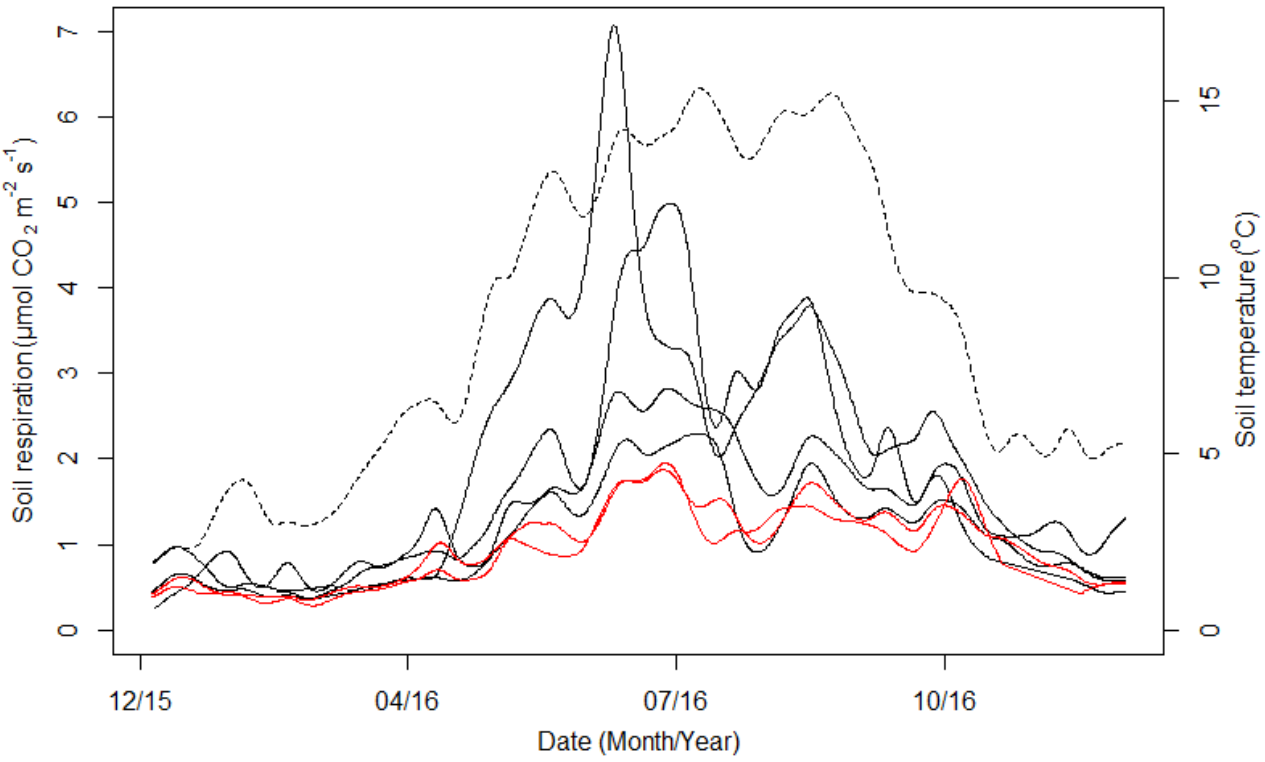


908

909 **Figure 3:** $R_{soil}$ (solid lines) throughout the year measured by the automated closed-chambers and
910 soil temperature at 5 cm depth (dashed line). The black solid lines show the $R_{soil}$ for the four plots
911 with intact soil and the red solid lines show $R_{soil}$ for the two plots with trenched soil. The lines have
912 been smoothed to show a running five day average.

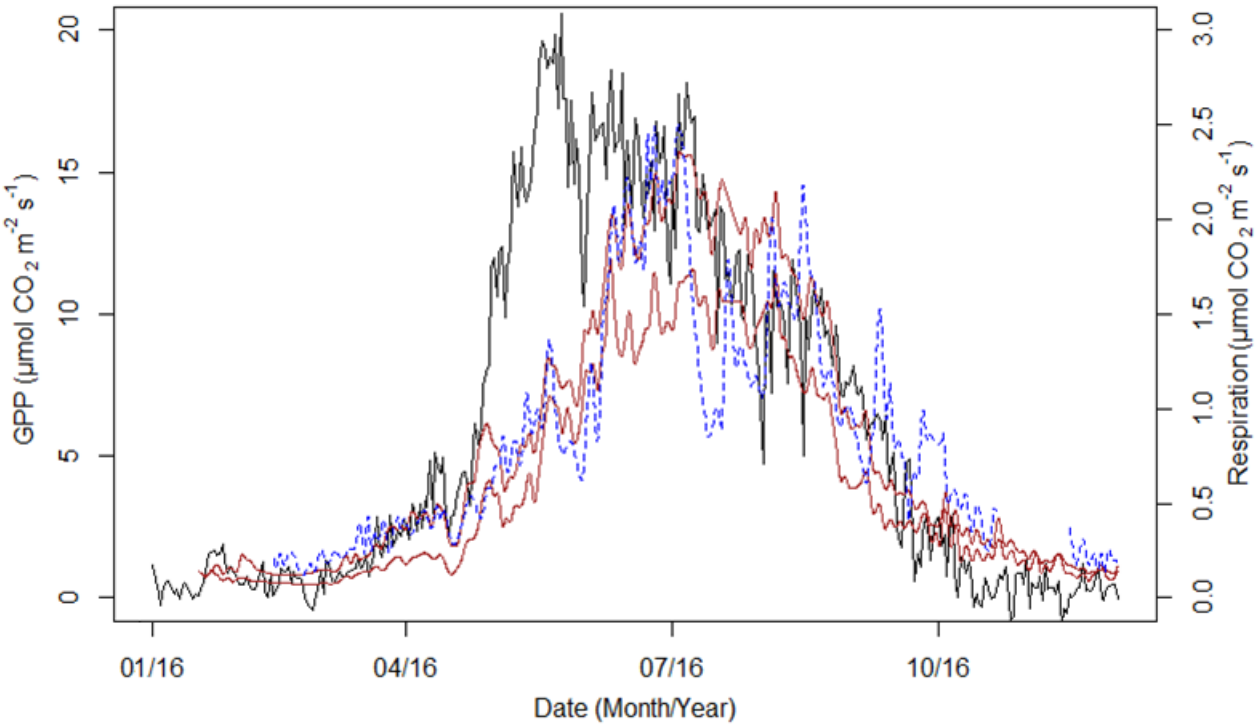


913

914 **Figure 4:** Mean daily GPP (black line, left y-axis) and $R_{stem}$ (the red lines, right y-axis) throughout
915 the year. For $R_{stem}$ both plots are shown. The blue dashed line shows the mean daily $R_{soil}$ for the
916 intact soil plots measured by the automated closed-chambers. $R_{soil}$ have been multiplied with 0.45 to
917 fit the right respiration scale.

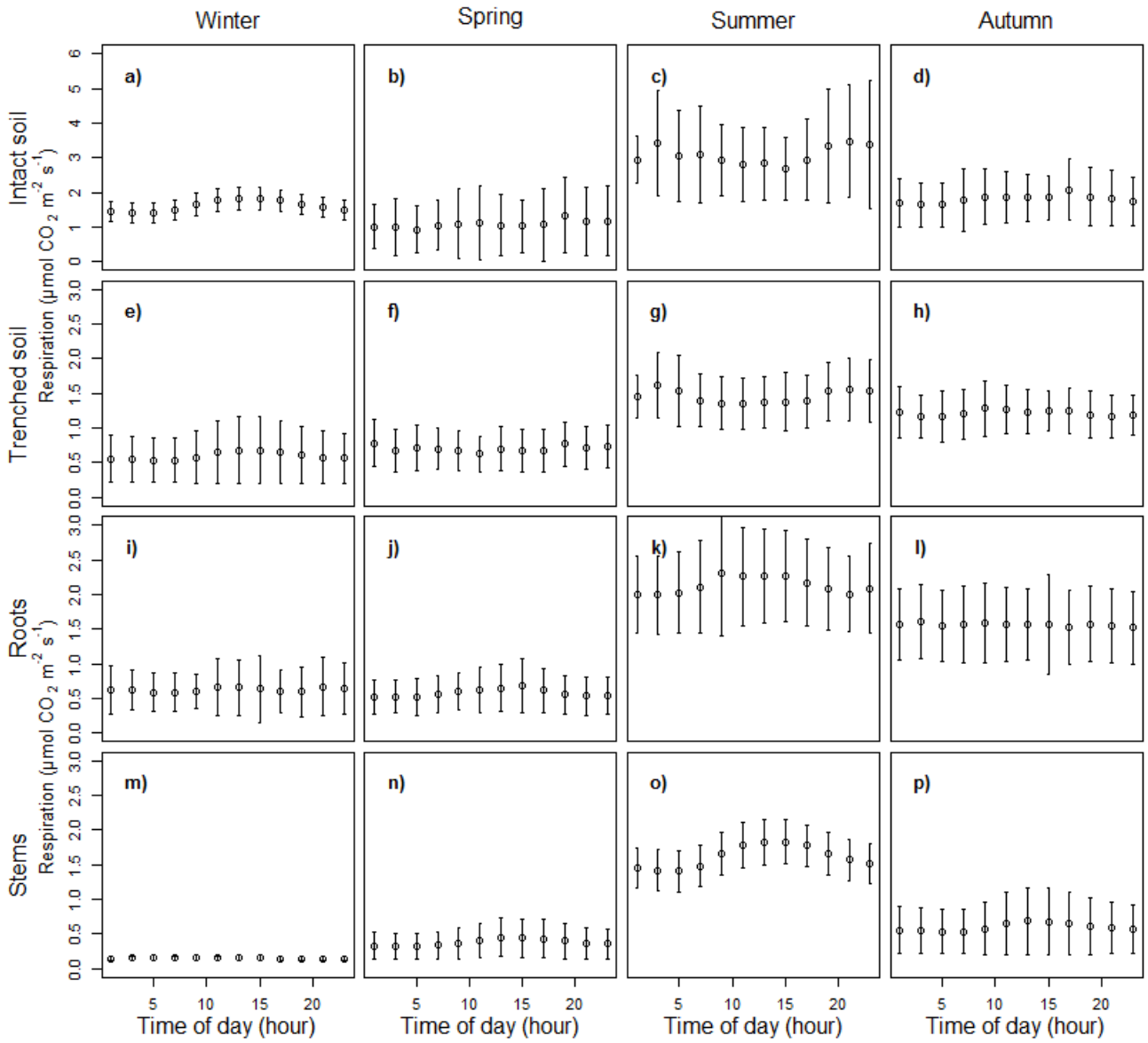


**Figure 5:** Seasonally averaged diel patterns of $R_{soil}$ for the intact and trenched soil, $R_{root}$ and $R_{stem}$ measured by the automated closed-chambers for each of the four seasons. Error bars show standard deviation. The seasons of winter, spring, summer and autumn are shown in the four columns from left to right, respectively. The four rows from top to bottom show $R_{soil}$ from intact soil, $R_{soil}$ from trenched soil, $R_{root}$ and $R_{stem}$, respectively. $R_{soil}$ is shown on a soil surface area basis, while $R_{root}$ and $R_{stem}$ are shown on root surface area and stem surface area basis, respectively.

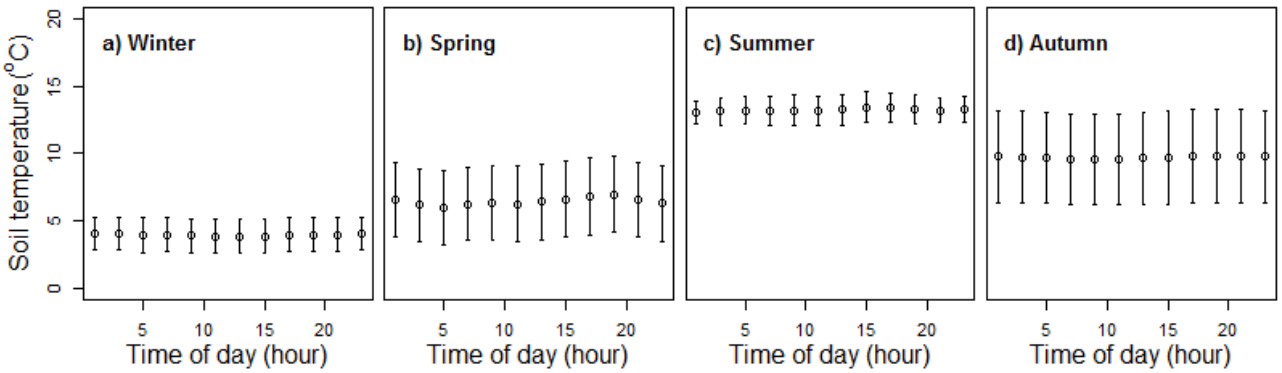


925

926 **Figure 6:** Seasonally averaged diel pattern of soil temperature (± standard deviation) at 5 cm depth
927 measured by soil thermometers installed close to the automated chambers for winter (a), spring (b),
928 summer (c) and autumn (d).